Biosensors and Bioelectronics 56 (2014) 300–306

Contents lists available at ScienceDirect

Biosensors and Bioelectronics

journal homepage: www.elsevier.com/locate/bios

CTAB functionalized graphene oxide/multiwalled carbon nanotube composite modified electrode for the simultaneous determination of ascorbic acid, dopamine, uric acid and nitrite

Yu Jun Yang [a,*], Weikun Li [b]

[a] School of Chemistry and Chemical Engineering, Xuchang University, Xuchang, Henan 461000, China
[b] University Library, Xuchang University, Xuchang, Henan 461000, China

ARTICLE INFO

Article history:
Received 30 December 2013
Received in revised form
19 January 2014
Accepted 20 January 2014
Available online 30 January 2014

Keywords:
Biosensor
Graphene oxide
Uric acid
Ascorbic acid
Dopamine
Nitrite

ABSTRACT

We have developed hexadecyl trimethyl ammonium bromide (CTAB) functionalized graphene oxide (GO)/multiwalled carbon nanotubes (MWNTs) modified glassy carbon electrode (CTAB-GO/MWNT) as a novel system for the simultaneous determination of dopamine (DA), ascorbic acid (AA), uric acid (UA) and nitrite (NO_2^-). The combination of graphene oxide and MWNTs endow the biosensor with large surface area, good biological compatibility, electricity and stability, high selectivity and sensitivity. In the fourfold co-existence system, the linear calibration plots for AA, DA, UA and NO_2^- were obtained over the range of 5.0–300 μM, 5.0–500 μM, 3.0–60 μM and 5.0–800 μM with detection limits of 1.0 μM, 1.5 μM, 1.0 μM and 1.5 μM, respectively. In addition, the modified biosensor was applied to the determination of AA, DA, UA and NO_2^- in urine samples by using standard adding method with satisfactory results.

1. Introduction

Dopamine (DA), ascorbic acid (AA), uric acid (UA) and nitrite ion (NO_2^-) usually coexist in biological matrixes, and they were considered as crucial molecules for physiological processes in human metabolism. DA is a neurotransmitter that is widely distributed in the mammalian central nervous system for message transfer, and it plays an important role in the function of the central nervous, renal and hormonal systems (Alarcon-Angelesa et al., 2008; Demier et al., 1999; El-Said et al., 2010). AA is another important component in human diet, and it plays a vital role in neurochemistry, bioelectrochemistry and clinical diagnostics applications (Koshiishi and Imanari, 1997). More importantly, it has been used for prevention and treatment of scurvy, mental illness and cancer (Noroozifar and Motlagh, 2003). Uric acid (UA) is the principal final product of purine metabolism, and it is an important biomolecule present in urine and blood. Elevated uric acid levels in the urine may indicate spreading cancer, consumption of a purine-rich diet, gout, Lesch–Nyhan syndrome, rhabdomyolysis and Fanconi syndrome (Dutt and Mottola, 1974). In recent years, many papers reported that NO could act as a neurotransmitter or a neuromodulator in the central nervous system. Although the physiological results of NO for DA release in the striatum are controversial, it is undisputed that NO can be oxidized to NO_2^- in biological circumstance as fast as in a few seconds (Garthwaite, 1991; Lonart et al., 1993; Zhang et al., 2011). Therefore, simultaneous determination of AA, DA, UA and NO_2^- is important for investigating their physiological functions and diagnosing diseases.

In the past few decades, electrochemical techniques have been received considerable interest for the detection of small biomolecules because of their high sensitivity, rapid response, simple operation, and low expense (Zhao et al., 2005). However, the oxidation potentials of these electroactive species are too close to be determined separately at bare glassy carbon electrode (GCE) which results in poor sensitivity and selectivity (Tang et al., 2008).

AA and DA were simultaneously determined with cobalt-5-nitrosalophen/tetraoctylammonium bromide/carbon-paste electrode (CPE) (Shahrokhian and Mehrjardi, 2007), poly(acriflavine)/GCE (Nien et al., 2009). UA and AA were simultaneously determined with electrodes modified with gold nanoparticles (NPs) (Kannan and John, 2009; Hu et al., 2008). AA, UA and DA were simultaneously determined with MWNT/poly(neutral red)/GCE (Yogeswaran and Chen, 2007), poly(eriochrome black T)/GCE (Yao et al., 2007), tetrabromo-p-benzoquinone/CPE (Zare et al., 2005), poly(mordant blue 13)/GCE (Ensafi et al., 2009), silver hexacyanoferrate/MWNT/GCE (Meissam et al., 2010), Fe_3O_4 NPs/reduced graphene oxide (rGO)/GCE (Teymourian et al., 2013), poly (acid chrome blue K)/GCE (Zhang et al., 2009), poly(Sulfonazo III)/

* Corresponding author. Tel.: +86 374 2968851.
E-mail address: yangyujun@yahoo.com (Y.J. Yang).

0956-5663/$ - see front matter © 2014 Elsevier B.V. All rights reserved.
http://dx.doi.org/10.1016/j.bios.2014.01.037

GCE (Ensafi et al., 2010), palladium NP-loaded carbon nanofibers/CPE (Huang et al., 2008), and carbon nanofibers/CPE (Liu et al., 2008). DA, UA and nitrite were simultaneously determined with graphene/poly-cyclodextrin/MWNT/GCE (Zhang et al., 2011). AA, UA, DA and nitrite were simultaneously determined with iron(III)-porphyrin/MWNT/GCE (Wang et al., 2012), lanthanum-MWNT/GCE (Zhang et al., 2012), Au NPs incorporated poly(3-amino-5-mercapto-1,2,4-triazole)/GCE (Wang et al., 2011). Although various materials have been utilized to modify electrodes in order to resolve the above problem, developing a facile method to simultaneously determine AA, DA, UA and nitrite is still a challenge.

Recently, a new two-dimensional (2D) carbon material, graphene attracts much attention in fabricating electrochemical biosensors (Alwarappan et al., 2012) because of its unique properties such as exceptional thermal and mechanical properties, large surface-to volume ratio and high electrical conductivity. The precursor for preparing the chemically reduced graphene, graphene oxide (GO) shows good hydrophilicity and dispersibility in water because it contains a large number of hydrophilic functional groups, such as OH, COOH and epoxides on the basal plane and the sheet edge. Although the conductivity of GO is not as high as graphene, it is also regarded as a suitable candidate for biosensing analysis (Alwarappan et al., 2012; Li et al., 2008, 2010; He et al., 2010; Du et al., 2011). Taking advantage of the above characteristics, we use CTAB-functionalized GO (CTAB-GO) and multiwalled carbon nanotubes (MWNTs) to construct sensing interface to achieve simultaneous detection of DA, AA, UA, and NO_2^-. Due to the combination of the advantages of GO and MWNT, the sensor exhibited excellent catalytic activity to DA, AA, UA and NO_2^-, which could facilitate the discrimination of many species with similar redox potentials. The attractive response performances of the proposed method and potential merits are presented in details.

2. Experimental

2.1. Reagents and materials

All chemical reagents were of analytical grade and used as received. Uric acid (UA) was purchased from Sigma Chemical Co. (St. Louis, MO, USA). Sodium nitrite ($NaNO_2$), ascorbic acid (AA) and dopamine (DA) were purchased from Sinopharm Chemical Reagent Co. Ltd. 0.1 M pH 7.0 phosphate buffer solutions were prepared using 0.1 M Na_2HPO_4 and 0.1 M NaH_2PO_4. Double-distilled water was used throughout the experiment.

2.2. Preparation of GO

GO was prepared from natural graphite by a modified Hummers method. Briefly, graphite powder (2 g) and $NaNO_3$ (1 g) were mixed, then it was put into 96 mL concentrated H_2SO_4 with an ice bath. Under vigorous stirring, 6 g $KMnO_4$ (99.6%) was added gradually. The temperature of the mixture was maintained below 20 °C. After removing the ice bath, the mixture was stirred at 35 °C in a water bath for 18 h. As the reaction extended, the mixture turned out to be pasty with a brownish color. Successively, 240 mL of H_2O was moderately added to the paste under stirring in an ice bath. Addition of water into the concentrated H_2SO_4 medium releases a large amount of heat. 5 mL of 30% H_2O_2 was added to the mixture, and the diluted solution color was transformed to brilliant yellow along with bubbling. After continuous stirring for 2 h, the mixture was subjected to 30 min of centrifugation at 4000 rpm and brown precipitate (graphene oxide) was collected. The precipitate was redispersed into 250 mL 10% HCl aqueous solution under ultrasonic agitation for 30 min and then isolated from aqueous phase by filtration. The obtained product cake was washed with 0.1 M HCl aqueous solution (1 L) to remove metal ions (like Mn^{2+}) followed by 250 mL dionized water to remove the acid by filter paper and funnel. The resulting solid was dried by vacuum and diluted to make graphite oxide stock dispersion (10 mg/mL). Finally, it was purified by dialysis for one week to remove the remaining ion species. Required concentration of graphene oxide dispersion was obtained by dispersing graphite oxide stock dispersion into water by ultrasonication for 1 h.

2.3. Preparation of CTAB-GO/MWNT suspension

CTAB-GO/MWNT was prepared by following steps: graphene oxide (15 mg) was dispersed into 50 mL water with 30 mg CTAB under ultrasonic agitation for4 h. The suspension was let stand for 12 h and allowed to separate into layers. Centrifuge the obtained CTAB-GO suspension at 4000 rpm. The precipitate was collected, washed copiously with water for several times and redispersed into 10 mL 0.2% chitosan 1% acetic acid solution with 10.1 mg MWNT under ultrasonic agitation for 2 h.

2.4. Fabrication of the sensor

To obtain mirror-like surface, the GCE (Φ=3 mm) was firstly polished successively with 0.3 and 0.05 μm alumina slurry. Then, it was rinsed with double distilled water and ethanol in ultrasonic bath to remove the physically absorbed substance. After that, the GCE was allowed to dry at room temperature. To construct the CTAB-GO/MWNT modified GCE, 10 μL of the CTAB-GO/MWNT suspension was dropped onto the surface of the GCE to fabricate a sensor (CTAB-GO/MWNT/GCE). Subsequently, it was dried in air. For comparison, MWNTs were dispersed in 0.2% chitosan 1% acetic acid solution and dropped onto the surface of the GCE to fabricate MWNT/GCE.

2.5. The physical and electrochemical measurements

Cyclic voltammetry (CV) was performed on CHI 660B (Chenhua, Shanghai). A three-electrode system comprising of a platinum wire as the auxiliary, a saturated calomel electrode (SCE) as the reference and the modified GCE as the working electrode was used for the electrochemical experiments. Infrared spectra (IR) were collected with a Fourier transform infrared (FT-IR) spectrophotometer (Vector 22, Bruker, Germany) using KBr disks. The morphology of the graphene film was observed with a scanning electron microscope (SEM). The crystalline structure of the graphene film was investigated with an X-ray diffractometer (XRD). The X-ray diffraction (XRD) patterns are obtained by Shimadzu XRD-6000 diffractometer with a Ni filter and Cu Kα radiation (λ=1.54056 Å). SEM experiments were carried out employing Quanta 200 scanning electron microscope (SEM; FEI Company, Holland).

3. Results and discussion

Fig. 1 shows FT-IR spectra of CTAB, CTAB-GO and GO. In comparison with that of GO, the absorption band of CTAB-GO at 1134 cm^{-1} (C–O–C stretching vibrations) is significantly diminished, indicating the reaction between CTAB and the epoxy group of GO. For CTAB-GO, the bands at 2924 cm^{-1} and 2853 cm^{-1} (C–H stretching vibrations) are designated to the characteristic absorption bands of CTAB main chain.

The surface morphologies of different modified electrodes were analyzed by scanning electron microscopy (SEM). Fig. 2A and B depictured the SEM micrographs of CTAB-GO/GCE and CTAB-GO/MWNT/GCE, respectively. As shown in Fig. 2a, the CTAB-GO film

appears a homogeneous surface which exhibits a wrinkled texture associating with the presence of flexible and ultrathin grapheme oxide sheets. However, the SEM image of CTAB-GO/MWNT film clearly shows the presence of numerous well distributed carbon nanotubes (Fig. 2b). In comparison with the rather smooth and even surface of CTAB-GO/GCE, the combination of MWCNTs with CTAB-GO leads to the formation of a highly porous 3 dimensional nanohybrid structure.

The cyclic voltammograms (CVs) of different modified electrodes in 0.1 M PB solution (pH 7.0) containing 1×10^{-3} M AA, 1×10^{-4} M DA, 1×10^{-4} M UA and 1×10^{-4} M nitrite were investigated. At the bare GCE (Fig. 3, curve b), the oxidation peaks of AA, DA, UA and nitrite completely overlap and a broad oxidation peak were observed at 0.5 V, which revealed that it is impossible to simultaneously determine these compounds. For CTAB-GO/GCE (Fig. 3, curve d), the peak currents of DA, AA, UA and nitrite were notably improved and the selectivity was better than that at the bare GCE. The anodic peaks at 0.1 V, 0.39 V and 0.83 V can be attributed to the oxidation of AA, UA and nitrite, respectively. However, simultaneous determination of AA, DA, UA and nitrite could not be obtained at CTAB-GO/GCE due to the indistinguishable and small response to DA.

Fig. 4 displays the cyclic voltammograms of the mixture of AA, DA, UA and nitrite at MWNT modified GCE (Fig. 4, curve b) and CTAB-GO/MWNT modified GCE (Fig. 4, curve d). At the MWNT/GCE, the peaks of DA and UA oxidation were observed at 0.19 V and 0.3 V, respectively, but the anodic peaks of AA and nitrite were inconspicuous and small. At CTAB-GO/MWNT/GCE, the voltammetric peaks of AA, DA, UA and nitrite appear at 0.01 V, 0.22 V, 0.31 V and 0.79 V, respectively, which make it possible to achieve the simultaneous determination of AA, DA, UA and nitrite.

The mechanisms behind the oxidation of AA, DA, UA and NO_2^- at a wide potential separation at CTAB-GO/MWNT/GCE are concluded in the following aspects. The combination of 1 dimensional MWNTs and 2 dimensional CTAB-GO formed a 3 dimensional hierarchical structure which makes the surface of CTAB-GO/MWNT/GCE more porous than that of CTAB-GO/GCE. According to Compton's suggestion that the conducting porous layers on the surface of electrodes can change the mass transport regime from linear (planar) diffusion to one of approximately 'thin layer' character and that this alternation can facilitate the discrimination

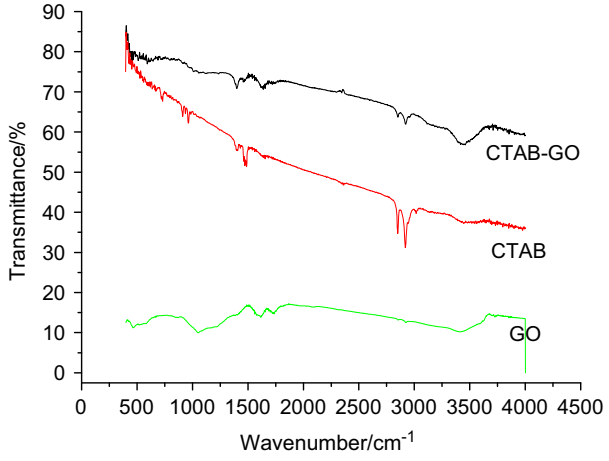

Fig. 1. The FT-IR spectra of GO, CTAB and CTAB-GO.

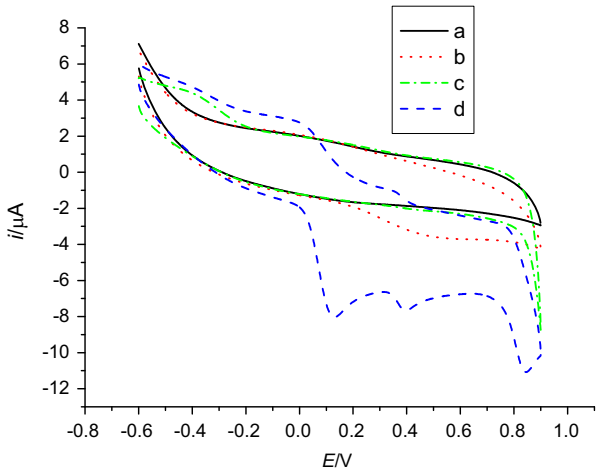

Fig. 3. Bare GCE in 0.1 M PB solution (pH 7.0) in the absence (a) and presence (b) of 1×10^{-3} M AA, 1×10^{-4} M DA, 1×10^{-4} M UA and 1×10^{-4} M nitrite; CTAB-GO/GCE in 0.1 M PB solution (pH 7.0) in the absence (c) and presence (d) of 1×10^{-3} M AA, 1×10^{-4} M DA, 1×10^{-4} M UA and 1×10^{-4} M nitrite.

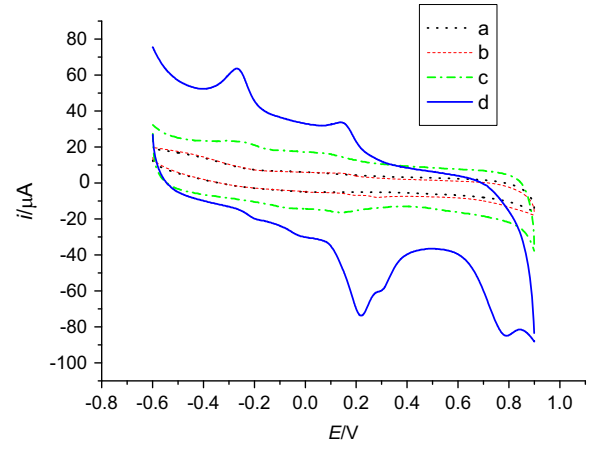

Fig. 4. MWNT/GCE in 0.1 M PB solution (pH 7.0) in the absence (a) and presence (b) of 1×10^{-4} M AA, 5×10^{-5} M DA, 1×10^{-4} M UA and 1×10^{-4} M nitrite; CTAB-GO/MWNT/GCE in 0.1 M PB solution (pH7.0) in the absence (c) and presence (d) of 1×10^{-3} M AA, 1×10^{-4} M DA, 1×10^{-4} M UA and 1×10^{-4} M nitrite.

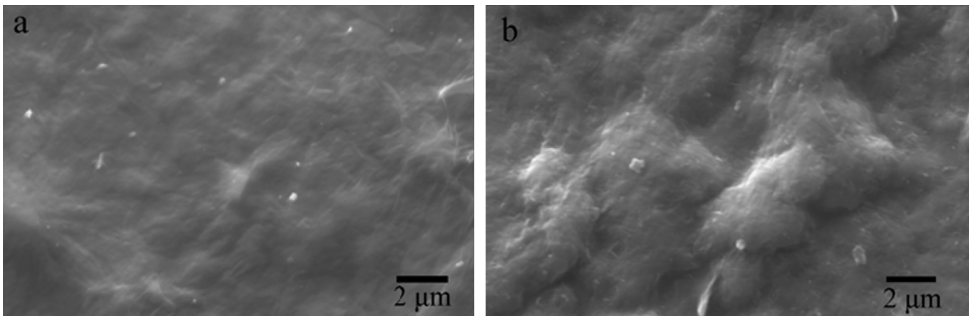

Fig. 2. SEM images of the (a) CTAB-GO/GCE and (b) CTAB-GO/MWNT/GCE.

of many species which oxidize or reduce at similar potentials (Henstridge et al., 2010).

The effect of pH on the CV response to the electro-oxidation of AA, DA, UA and nitrite in PB solution at CTAB-GO/MWNT/GCE was studied over the pH range 6–8 (Fig. 5). At pH 6.0, the anodic peaks at 0.01 V, 0.26 V, 0.33 V and 0.80 V can be attributed to the oxidation of AA, DA, UA and nitrite, respectively. However, the oxidative peak of DA is very small and barely observable. As the solution pH was increased from 6.0 to 7.0, the anodic peak currents of DA and UA were increased significantly while the anodic peak currents of AA and nitrite were decreased. Further increase of the solution pH from 7.0 to 8.0, the anodic peak currents of AA and nitrite were increased while the anodic peak current of DA was decreased and the anodic peak of UA was barely observable. Since, considering the conditions of application, pH 7.0 was selected as the pH value of supporting electrolyte in the simultaneous detection of AA, DA, UA and nitrite.

Fig. 6 demonstrated the effect of scan rates on the electrochemical response of AA, UA, DA and nitrite using cyclic voltammetry. The anodic peak currents at 0.01 V, 0.22 V, 0.31 V and 0.79 V were proportional to the square root of the scan rate ($v^{1/2}$). Linear relationship between the catalytic peak current and the square root of scan rate indicated that the oxidations of AA, UA, DA and nitrite on CTAB-GO/MWNT/GCE were diffusion controlled processes.

Fig. 7 depicts the DPV recordings at various concentrations of AA, DA, UA and nitrite at CTAB-GO/MWNT/GCE. In the presence of AA, an anodic peak at −0.07 V was observed which is ascribed to the oxidation of AA (Fig. 7, curve a). After the addition of UA, one more peak at 0.24 V was observed, which was attributed to the oxidation of UA (Fig. 7, curve b). As shown in Fig. 7curve c, the anodic peak at 0.16 V is due to the oxidation of DA. Four well-defined separated anodic peaks corresponding to oxidation of AA, DA, UA and nitrite are observed at potentials of approximately −0.07 V, 0.17 V, 0.24 V and 0.73 V, respectively (Fig. 7, curve d).

The oxidation peak currents of these four molecules linearly increased with their concentrations (Fig. 8a). For AA (Fig. 8b), the linear regression equations is obtained which is expressed as i_{AA} (μA)= −28.356–0.08186[AA] (μM) ([AA]: 5.0–300.0 μM, R^2= 0.99901). For DA (Fig. 8c), the linear regression equations is obtained which is expressed as i_{DA} (μA)= −25.24333–0.21739[DA] (μM) ([DA]: 5.0–500.0 μM, R^2=0.99866). In the case of UA (Fig. 8d), two linear regression equations were also obtained which are calculated as i_{UA} (μA)= −38.143–0.2372[UA] (μM) ([UA]: 3.0–60.0 μM, R^2=0.99686) and i_{UA} (μA)= −23.09133–0.52349[UA] (μM) ([UA]: 70.0–500 μM, R^2=0.99589). For nitrite (Fig. 8e), the linear regression equations was expressed as $i_{nitrite}$ (μA)= −29.20856–0.10273[NO_2^-] (μM) ([NO_2^-]: 5.0–800 μM, R^2=0.99426). The detection limits (LOD) were calculated using the common formula LOD=3σ/S, where σ is the standard deviation from the blank measurement and S is the

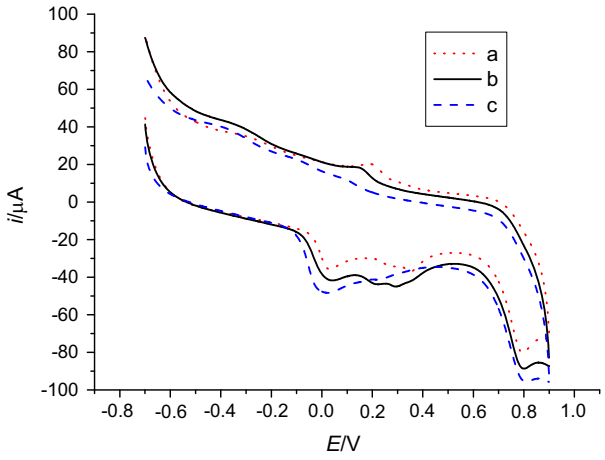

Fig. 5. CV responses of 1 mM AA, 3×10^{-5} M DA, 5×10^{-5} M UA and 1×10^{-4} M nitrite in 0.1 M PB buffer solution at various pH values: pH6.0 (solid line), pH7.0 (dotted line), and pH 8.0 (dash-dotted line) at CTAB-GO/MWNT/GCE.

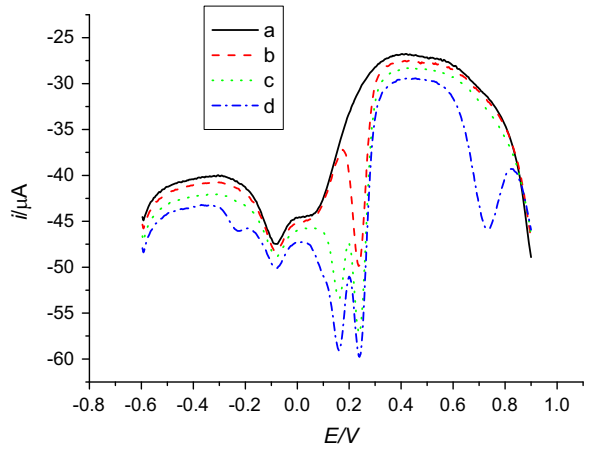

Fig. 7. DPVs of CTAB-GO/MWNT/GCE in 0.1 M PB solution (pH 7.0) containing (a) 1×10^{-4} M AA, (b) 1×10^{-4} M AA and 1×10^{-4} M UA, (c) 1×10^{-4} M AA, 5×10^{-5} M UA and 1×10^{-4} M DA, and (d) 1×10^{-4} M AA, 5×10^{-5} M UA, 1×10^{-4} M DA and 1×10^{-4} M nitrite.

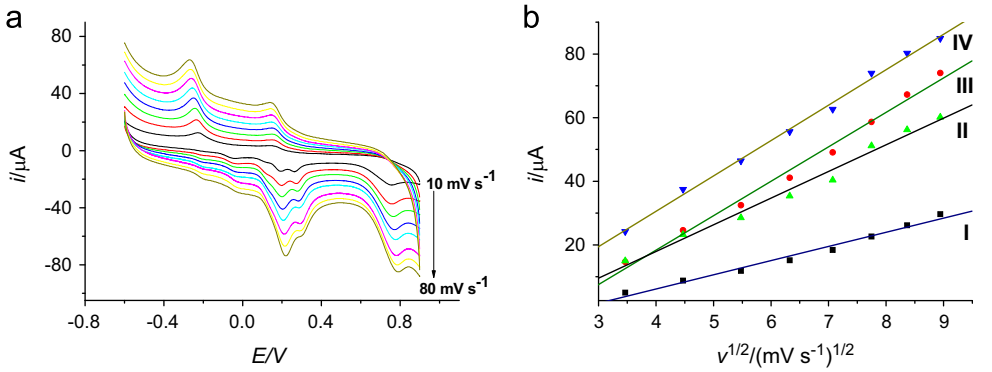

Fig. 6. (a) Cyclic voltammograms at 10, 20, 30, 40, 50, 60, 70, and 80 mV/s on CTAB-GO/MWNT/GCE in the presence of 1×10^{-4} M AA, 5×10^{-5} M DA, 1×10^{-4} M UA and 1×10^{-4} M nitrite in 0.1 M pH 7.0 PBS and (b) the anodic peak currents of AA (I), DA (II), UA (III) and nitrite (IV) *vs.* the square root of scan rate.

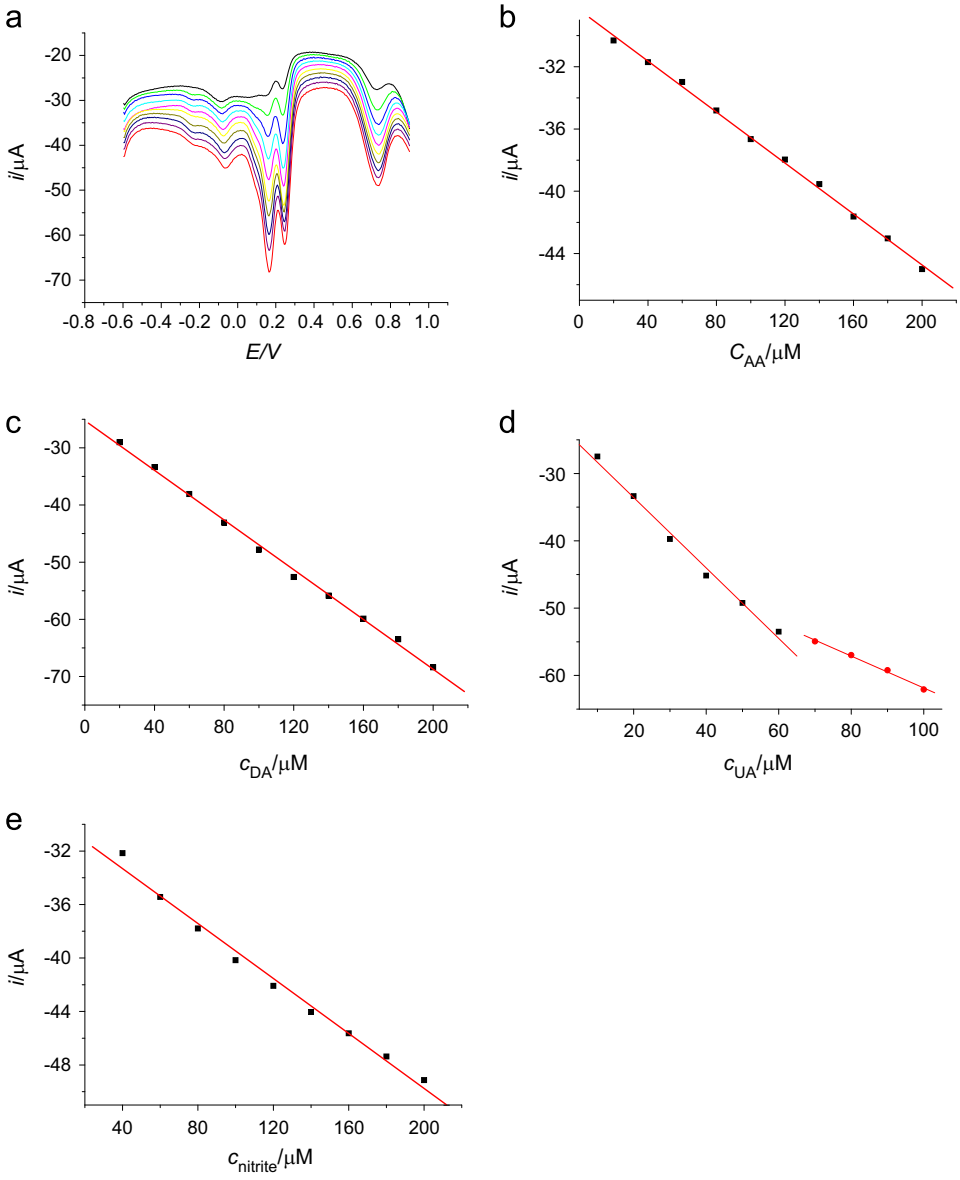

Fig. 8. (a) DPVs of CTAB-GO/MWNT/GCE in PB solution (0.1 M, pH 7.0) containing mixed concentrations of the AA, DA, UA and nitrite mixture. [AA]: 20.0, 40.0, 60.0, 80.0, 100.0, 120.0, 140.0, 160.0, 180.0 and 200.0 μM. [DA]: 20.0, 40.0, 60.0, 80.0, 100.0, 120.0, 140.0, 160.0, 180.0 and 200.0 μM. [UA]:10.0, 20.0, 30.0, 40.0, 50.0, 60.0, 70.0, 80.0, 90.0 and 100.0 μM. [NO_2^-]: 20.0, 40.0, 60.0, 80.0, 100.0, 120.0, 140.0, 160.0, 180.0 and 200.0 μM. (b) Plot of oxidation peak currents *vs.* the concentration of AA; (c) the plot of oxidation peak currents *vs.* the concentration of DA; (d) the plot of oxidation peak currents *vs.* the concentration of UA and (e) the plot of oxidation peak currents *vs.* the concentration of nitrite.

Table 1
Comparison of performances of proposal sensor for the detection of AA, DA, UA and NO_2^- with those of sensors based on different matrices.

Electrode	Method	Linear response range (μM)				Limit of detection (μM)				Ref.
		AA	DA	UA	NO_2^-	AA	DA	UA	NO_2^-	
Graphene/polycyclodextrin/ MWNT/GCE	DPV	5–480	0.15–21.65	–	5–6750	1.65	0.05	–	1.65	Zhang et al. (2011)
Poly(acid chrome blue K)/GCE	DPV	50–1000	1.0–200	1.0–120	–	10.0	0.5	0.5	–	Zhang et al. (2009)
Poly(eriochrome black T)/GCE	DPV	150–1000	0.1–200	10–130	–	10.0	0.02	1.0	–	Yao et al. (2007)
Poly-sulfonazo III /GCE	DPV	0.5–1300	0.05–470	0.2–100	–	0.17	0.03	0.11	–	Ensafi et al. (2010)
Poly-CDDA/ GCE	DPV	5.0–240	5.0–280	0.1–18	–	1.43	0.29	0.016	–	Ensafi et al. (2009)
GNP/LC/GCE	DPV	6.0–850	–	8.0–550	–	3.0	–	0.2	–	Hu et al. (2008)
Pd/CNF-CPE	DPV	50–4000	0.5–160	2–200	–	15	0.2	0.7	–	Huang et al. (2008)
Carbon nanofiber-CPE	DPV	2–64	0.04–5.6	0.8–16.8	–	2	0.04	0.2	–	Liu et al. (2008)
Fe(III)P/MWNT	*CA*	14–250	0.7–360	5.8–130	–	3.0	0.09	0.3	–	Kalimuthu and John (2009)
La/MWCNT	*CA*	0.4–71	0.04–89	0.04–81	0.4–71	0.14	0.01	0.015	0.13	Zhang et al. (2012)
Fe_3O_4/rGO/GC	DPV	160–722	0.4–3.5	20–212	–	20	0.08	0.5	–	Teymourian et al. (2013)
CTAB-GO/MWNT/GCE	DPV	5.0–300	5.0–500	3.0–60	5.0–800	1.0	1.5	1.0	1.5	This work

slope of the calibration curve. The detection limits for the determination of AA, DA, UA and nitrite were evaluated as 1.0 μM, 1.5 μM, 1.0 μM and 1.5 μM, respectively. The lowest detection limits obtained here for simultaneous determination of AA, DA, UA and nitrite are comparable or in some cases better than previously reported values. In Table 1, some of the analytical characteristics obtained in this work are compared with those previously reported in the literature.

The stability of the modified electrode was also studied in this work. When the electrode was cyclically swept for 10 cycles (Fig. S1), 0.9%, 0.7%, 1.1%, and 3.1% decrease of the initial responses of the modified electrode were observed, indicating that the CTAB-GO/MWNT/GCE had excellent stability. The reproducibility of the proposed biosensor was determined with 4 different electrodes. The relative standard deviations (RSD) of the current responses for AA, DA, UA, and NO_2^- were 3.3%, 3.1%, 2.7%, and 2.5%, respectively (Fig. S2).

In order to investigate the selectivity of the CTAB-GO/MWNT/GCE, several compounds from common co-existing substances were investigated by detecting the response of the modified electrode to AA, DA, UA and NO_2^-. Experimental results indicated that no interference was found from 100 μM glucose, 100 μM L-cysteine and 100 μM citric acid (Fig. S3).

The data on the normal levels of DA, AA and UA in human urine were provided by the Clinical Laboratory of Central Hospital (Xuchang City, Henan Province, PR China). Clinical test of DA measures the amount of DA in a urine sample that is collected over 24 h. Normal DA level ranges 0.424–2.612 μmol in a 24-hour urine collection. The UA concentration in urine ranges 149–416 μM for adult healthy men and 89–357 μM for adult healthy women. Urinary AA concentration ranges 0–0.6 mM in normal people. However, the level of urinary AA is not of clinical significance because it is dependent on the amount of AA orally taken by the body. The concentration ranges of DA, AA and UA in the urine of patient are unable to get due to the great variety of diseases. There is no data on the normal level of nitrite in human urine because the test on nitrite in urine is not a routine test.

Human urine samples were selected as biological samples for analysis using the standard addition method to evaluate the applicability of the proposed system. The proposed sensor was applied to test AA, DA, UA and nitrite in two urine samples. The human urine samples were diluted 50-fold with 0.1 M PBS without any other treatment. The dilution process can help to reduce the matrix effect of real samples. DPV response was measured after 200 μL human urine sample was added into 10 mL 1.0 M PB stock solution (pH 7.0). Only UA was detected in both urine samples. Since no AA, DA and nitrite was detected in the samples, certain amount (10 μL for sample 1 and 5 μL for sample 2) of spike solution containing 0.02 M AA, 0.02 M DA, 0.01 M UA and 0.02 M nitrite was added into the samples to check the recoveries of AA, DA, UA and nitrite. The percent recovery of the spike was calculated as follows:

$$\%R = \frac{(\text{spiked sample result} - \text{unspiked sample result})}{\text{known spike added concentration}} \times 100\%.$$

The recoveries of AA, DA, UA and nitrite all fall in 99–110%, validating that the proposed system is suitable for determination of AA, UA, DA and nitrite in real biological samples (Table 2).

Table 2
Determination results of AA, DA, UA and NO_2^- in real samples ($n=5$).

Sample		Analyte concentration in the unspiked sample (μM)	Known spike added concentration (μM)	Analyte concentration in the spiked sample (μM)	Recovery (%)
Urine 1	AA	–	20.0	21.5	107.5
	DA	–	20.0	21.9	109.5
	UA	5.0 ± 0.2	10.0	16.5	115
	NO_2^-	–	20.0	19.8	99
Urine 2	AA	–	10.0	11.0	110
	DA	–	10.0	10.8	108
	UA	3.9 ± 0.2	5.0	9.2	106
	NO_2^-	–	10.0	10.5	105

4. Conclusions

In conclusion, a biosensor has been fabricated based on the construction of a novel nanocomposite CTAB-GO/MWNT. The new hybrid material combines the electrocatalytic behavior of CTAB-GO with the excellent catalytic properties of MWNT. The resulting nanocomposite was investigated by various characterization methods, including FT-IR, XRD, and SEM. The biosensor not only exhibited high electrocatalytic activities towards the oxidation of AA, DA, UA and NO_2^-, but also resolved the overlapping peaks, lowered the overpotential, and greatly enhanced the current response because of the synergistic integration of the CTAB-GO and MWNT. Furthermore, compared with MWNT/GCE and CTAB-GO/GCE, the CTAB-GO/MWNT/GCE could facilitate the simultaneous determinations of AA, DA, UA and NO_2^- with high sensitivity and selectivity. CTAB-GO/MWNT hybrid could be an extremely promising candidate applicable for a wide range of electrochemical sensing and biosensing applications.

Appendix A. Supporting information

Supplementary data associated with this article can be found in the online version at http://dx.doi.org/10.1016/j.bios.2014.01.037.

References

Alarcon-Angelesa, G., Perez-Lopez, B., Palomar-Pardave, M., Ramırez-Silva, M.T., Alegret, S., Merkoci, A., 2008. Carbon 46, 898–906.
Alwarappan, S., Boyapalle, S., Kumar, A., Li, C.Z., Mohapatra, S., 2012. J. Phys. Chem. C 116, 6556–6559.
Demier, P., Hirsch, E.C., Agid, Y., Graybiel, A.M., 1999. Brain 122, 1437–1448.
Du, D., Wang, L.M., Shao, Y.Y., Wang, J., Engelhard, M.H., Lin, Y.H., 2011. Anal. Chem. 83, 746–752.
Dutt, V.S.E., Mottola, H.A., 1974. Anal. Chem. 46, 1777–1781.
El-Said, W.A., Lee, J.H., Oh, B.K., Choi, J.W., 2010. Electrochem. Commun. 12, 1756–1759.
Ensafi, A.A., Taei, M., Khayamian, T., 2009. J. Electroanal. Chem. 633, 212–220.
Ensafi, A.A., Taei, M., Khayamian, T., Arabzadeh., A., 2010. Sens. Actuators B 147, 213–221.
Garthwaite, J., 1991. Trends Neurosci. 14, 60–67.
He, S.J., Song, B., Li, D., Zhu, C.F., Qi, W.P., Wen, Y.Q., Wang, L.H., Song, S.P., Fang, H.P., Fan, C.H., 2010. Adv. Funct. Mater. 20, 453–459.
Henstridge, M.C., Dickinson, E.J.F., Compton, R.G., 2010. Sens. Actuators B 145, 417–427.
Hu, G.Z., Ma, Y.G., Guo, Y., Shao, S.J., 2008. Electrochim. Acta 53, 6610–6615.
Huang, J.S., Liu, Y., Hou, H.Q., You, T.Y., 2008. Biosens. Bioelectron. 24, 632–637.
Kalimuthu, P., John, S.A., 2009. Biosens. Bioelectron. 24, 3575–3580.
Kannan, P., John, S.A., 2009. Anal. Biochem. 386, 65–72.
Koshiishi, I., Imanari, T., 1997. Anal. Chem. 69, 216–220.
Li, D., Muller, M.B., Gilje, S., Kaner, R.B., Wallace, G.G., 2008. Nat. Nanotechnol. 3, 101–105.
Li, F., Huang, Y., Yang, Q., Zhong, Z.T., Li, D., Wang, L., Song, S.P., Fan, C., 2010. Nanoscale 2, 1021–1026.
Liu, Y., Huang, J.S., Hou, H.Q., You, T.Y., 2008. Electrochem. Commun. 10, 1431–1434.
Lonart, G., Cassels, K.L., Johnson, K.M., 1993. J. Neurosci. Res. 35, 192–198.
Meissam, N., Mozhgan, K.M., Aboozar, T., 2010. Talanta 80, 1657–1664.
Nien, P.C., Chen, P.Y., Ho, K.C., 2009. Sens. Actuators B 140, 58–64.
Noroozifar, M., Motlagh, M.K., 2003. Talanta 61, 173–179.
Shahrokhian, S., Mehrjardi, H.R.Z., 2007. Sens. Actuators B 121, 530–537.
Tang, C.F., Kumar, S.A., Chen, S.M., 2008. Anal. Biochem. 380, 174–183.
Teymourian, H., Salimi, A., Khezrian, S., 2013. Biosens. Bioelectron. 49, 1–8.
Wang, C., Yuan, R., Chai, Y., Zhang, Y., Hu, F., Zhang, M., 2011. Biosens. Bioelectron. 30, 315–319.

Wang, C., Yuan, R., Chai, Y., Chen, S., Zhang, Y., Hu, F., Zhang, M., 2012. Electrochim. Acta 62, 109–115.
Yao, H., Sun, Y.Y., Lin, X.H., Tang, Y.H., Huang, L.Y., 2007. Electrochim. Acta 52, 6165–6171.
Yogeswaran, U., Chen, S.M., 2007. Electrochim. Acta 52, 5985–5996.
Zare, H.R., Nasirizadeh, N., Ardakani, M.M., 2005. J. Electroanal. Chem. 577, 25–33.
Zhang, R., Jin, G.D., Hu, X.Y., 2009. Sens. Actuators B 138, 174–181.
Zhang, Y., Yuan, R., Chai, Y.Q., Li, W.J., Zhong, X., Zhong, H., 2011. Biosens. Bioelectron. 26, 3977–3980.
Zhang, W., Yuan, R., Chai, Y.-Q., Zhang, Y., Chen, S.-H., 2012. Sens. Actuators B 166 (167), 601–607.
Zhao, Y.F., Gao, Y.Q., Zhan, D.P., Liu, H., Zhao, Q., Kou, Y., Shao, Y.H., Li, M.X., Zhuang, Q.K., Zhu, Z.W., 2005. Talanta 66, 51–57.